Acta of Bioengineering and Biomechanics
Vol. 16, No. 4, 2014

Original paper
DOI: 10.5277/ABB-00041-2014-02

Finite element analysis of the percutaneous coronary intervention in a coronary bifurcation

JAKUB KAROL BUKAŁA[1]*, JERZY MAŁACHOWSKI[1], PIOTR KWIATKOWSKI[2]

[1] Department of Mechanics and Applied Computer Science, Military University of Technology, Warsaw, Poland.
[2] Clinical Department of Interventional Cardiology, Central Clinical Hospital Ministry of Interior, Warsaw, Poland.

Purpose: The paper presents the process of numerical modeling and simulation of balloon angioplasty of the coronary artery using Finite Element Method.

Methods: The authors focused on the issue of applying adequate pressure in an arterial tissue during the post-dilatation process in the "kissing balloon" stenting technique applied to patients with bifurcation stenosis. Despite great progress in the field of interventional cardiology, angioplasty in bifurcations still belongs to the most difficult interventions, generally being less effective and more risky than in the cases of straight stenosis.

Results: During the modeling procedures and further simulations, the authors focused on mutual cooperation of non-compliant angioplasty balloons and the coronary artery. The other goal was to develop a sufficiently accurate model of the coronary artery fragment, including its bifurcation and angioplasty balloons; however, it was decided to ignore the modeling of coronary stents.

Conclusions: The issue undertaken is considered as relatively complicated and complex but, in the authors' opinion, the implementation of advanced computer aided engineering techniques may, in this case, answer several important questions without the need of performing costly and aggravating in vivo tests.

Key words: *angioplasty, balloon, FEA, kissing, simulation*

1. Introduction

Incessant progress that can be observed enabled invasive cardiologists to conduct the most difficult procedures especially within the area of bifurcation – the place of the origin of the side branch from the main artery. It can be estimated that all of them constitute about 15–20% of all PTCA (Percutaneous Transluminal Coronary Angioplasty) procedures [14], [24]. There are lots of techniques (such as mini crush technique, culotte, or provisional T stenting) applied to obtain the optimal, angiographic effect of the angioplasty [9]. Therefore, special stents and angioplasty balloons were developed. Their peculiar shape and construction made them irreplaceable in the field of bifurcation angioplasty [25], [29].

Understanding the causes of a miscarriage of the angioplasty according to the variety of the morphological views of bifurcations, shape and anatomy of the left main lesions, with different diameters of the main artery according to the side branch, plaque location, length, extension, morphology and angulations of the side branch origin, make it possible to apply a wide range of solutions that improve the effect of PTCA [28].

Bifurcation angioplasty is a very complex procedure, which relates to the main and side branch. Unfortunately, despite the unceasing progress in interventional cardiology especially in the range of the accessibility to the new equipment and new improved procedure techniques, outlying effects of the bifurcation angioplasty are still unacceptable. It is worth pointing out that bifurcation angioplasty is one of the

* Corresponding author: Jakub Karol Bukała, Department of Mechanics and Applied Computer Science, Military University of Technology, ul. gen. Sylwestra Kaliskiego 2, 00-908 Warsaw, Poland. Tel: +48 22 683 96 83, e-mail: jbukala@wat.edu.pl
Received: April 16th, 2014
Accepted for publication: April 21st, 2014

most difficult and advanced procedures in the field of interventional cardiology [1], [31], [12].

In the case of complications like restenosis or in stent thrombosis, which are infrequent but still occur, reangioplasty might be a necessity. Stent thrombosis can lead to the MACE (Major Adverse Cardiac Event) like death. Injury of the artery wall which activates a defensive response of the whole coronary system may be caused by the usage of incorrect equipment or false techniques according to the PTCA [22].

Therefore, it seems to be crucial to conduct extensive studies in the field of biomedical engineering. Research may contribute to the development of a new sophisticated appliance during conducting percutaneous interventions. The balance and cooperation between medical and engineering science efficiently influences progress in the methods of heart disease treatment. Thus, it improves comfort and life expectancy of a number of patients with the above mentioned problem.

The literature review made by the authors suggests that there are no papers in which the modeling methodology of balloon angioplasty of the coronary artery using Finite Element Method is extensively described. This fact and the remarks presented earlier were a direct cause to undertake the issue described in the paper.

The authors focused on the issue of mutual cooperation of two non-compliant angioplasty balloons and the coronary artery during the post-dilatation process in the "kissing balloon" stenting technique, applied to patients with bifurcation stenosis. The other goal was to develop a sufficiently accurate model of the coronary artery fragment, including its bifurcation and angioplasty balloons; however, it was decided to ignore the modeling of coronary stents.

2. Materials and methods

2.1. Geometry and discrete model of coronary bifurcation

Modeling the biological structures, in particular soft tissues, is a high complexity problem (geometry, material properties, etc.). In the paper, it was decided to create a sufficiently accurate model of the human coronary artery fragment, including its actual geometry and material parameters. It was necessary, however, to introduce certain simplifications that were imposed by restrictions of simulation methods and available computing resources.

It was decided that the initial model of the coronary arteries will be obtained by Computed Tomography (CT) imaging. Unfortunately, the accuracy of CT imaging depends strictly on the resolution of the machine. All these factors determined the fact that premapped geometry is further elaborated by Intravascular Ultrasound (IVUS) echo images.

CT images are monochrome and various shades of gray correspond to the respective values of the radiological density in the Hounsfield scale [16]. An image of the heart in a transverse plane with a marked place where the Left Coronary Artery (LCA) arises from the aorta is shown in Fig. 1. Finally, through interpolation in three dimensions between separated masks in Mimics®, a model of the left coronary artery with side branches was created (Fig. 1).

Intravascular ultrasound images were used to accurately reproduce the geometry of artery walls. It must also be added that IVUS survey is more reliable and more conclusive than computed tomography imaging when it comes to coronary arteries. Designated cross sections were reproduced as accurately as possible in CAE software in accordance with all measured dimensions. Afterwards they were placed in the appropriate position of the geometry model obtained by means of CT.

The profiles have been discretized in Altair Hyper Mesh software. At the outset, it was decided to opt out of 8-node solid elements for 4-node shell elements for the inner surface of the vessel. The result was a 44997 4-node quad element (fully integrated shell element) model, based on 44765 nodes. The thickness of elements in the transverse direction was set at 0.7 [mm], an average value for both the literature study and thickness specified in the IVUS survey [7], [8], [13], [16], [21], [23].

2.2. Angioplasty non-compliant balloon model

High pressure "non-compliant" balloons are made of materials characterized by a very small susceptibility. They allow the shape to be maintained despite the high pressure used to inflate. Balloons are made of "PET"-Polyethylene terephthalate and Nylon® [5]. The ideal balloons should be characterized by a very thin, non-compliance layer, with high durability and a small profile available in a wide range of length and diameter. It should be underlined that the shape (sometimes complex) and the presence of special coats on the balloon surface can be exerted during planning and formation process of new models of the balloons [5].

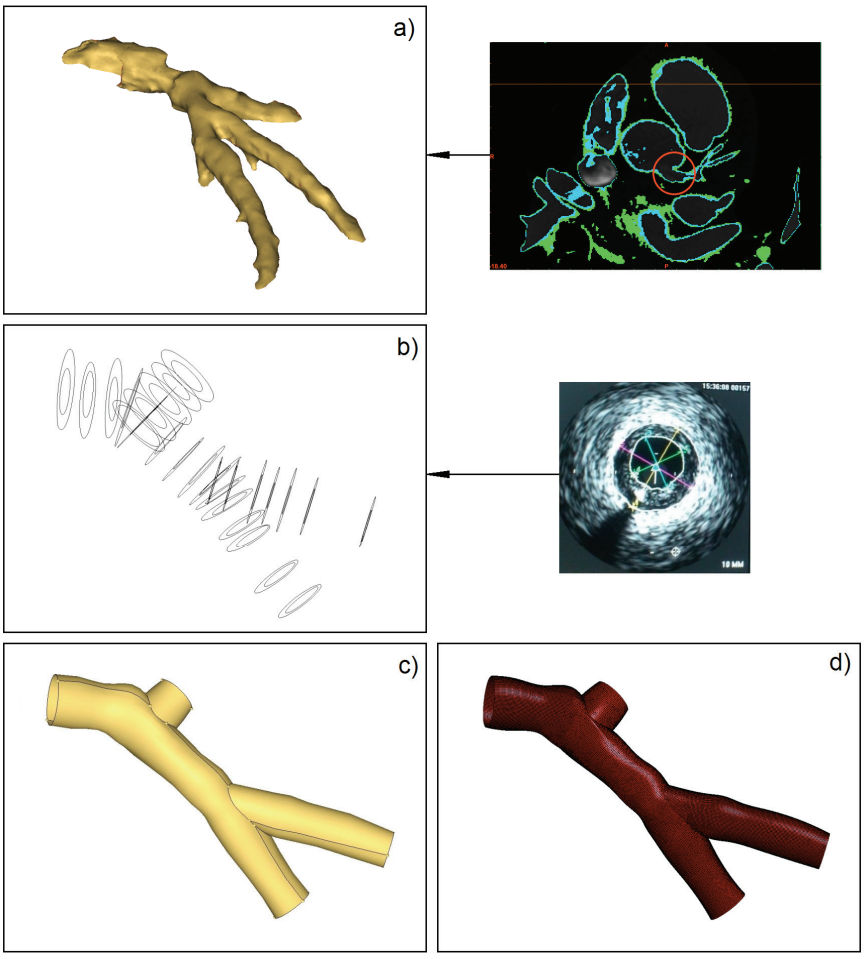

Fig. 1. Subsequent stages of developing the discrete model of coronary artery fragment: (a) three-dimensional artery volume reconstruction based on CT (red circle marks the spot where left coronary artery (LCA) arises from aorta); (b) image of detailed cross sections from IVUS survey; (c) geometrical model of the inner surface of the coronary artery; (d) discrete model – 2D shell elements

The process of developing the balloons geometry took several aspects into account:

- the shape of the inflated balloon (a classic balloon with a cylindrical body and a conical sharp endings was chosen);
- the non-compliant balloon folded form (the common three wings type);
- shape (facing) of the inflated balloon in the coronary artery (particularly important in terms of location of the two balloons within the vessel without initial collision).

It was decided to model the balloon geometry in a compressed form (as opposed to many works on a similar topic, where the geometry of the compressed balloon was pre-simulated from an inflated form [6], [18]). After the analysis of the geometry fragment of the coronary artery, the most appropriate dimensions for the two balloons were chosen:

- main branch (body length: 10 [mm], total length: 15 [mm],
- inflated balloon diameter 2 [mm], compressed balloon diameter: 1 [mm]);
- side branch (body length: 10 [mm], total length: 15 [mm],
- inflated balloon diameter 1,5 [mm], compressed balloon diameter: about 0.8 [mm]);

Discretization of the main branch balloon and the side branch balloon was based on 47 250 and 35 000 4-node 2D shell elements, respectively. In both cases, the elements were formulated as fully integrated shell elements, and they were given a thickness of 0.02 [mm].

2.3. Constitutive modelling

There are numerous works on the material models and material constants of the coronary artery tissue [7], [21], [26]. In the paper, the artery material was based on a 5-parametric hyperelastic model, based on the strain energy density function according to the

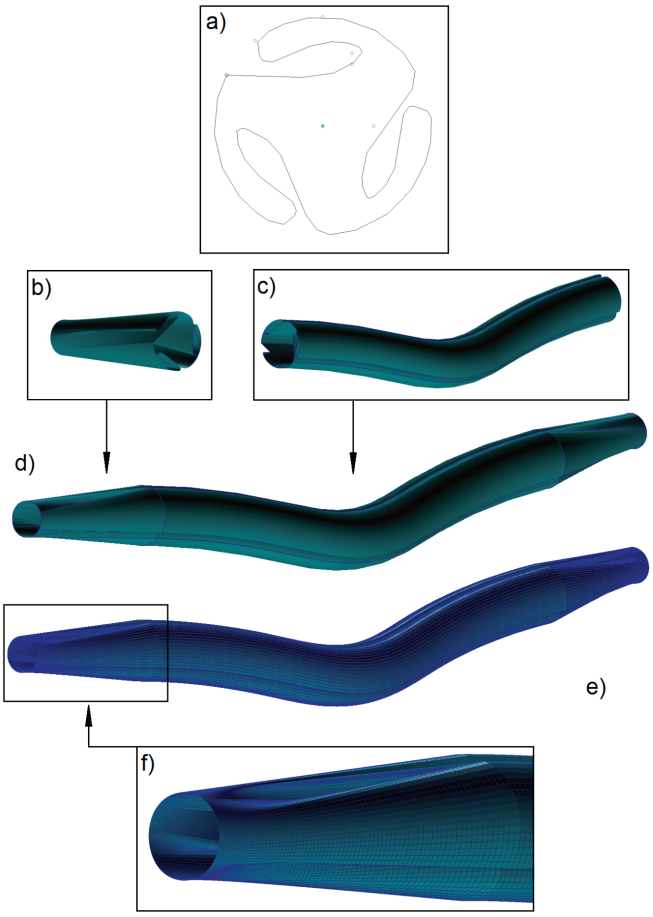

Fig. 2. Geometrical model and finite element mesh of the proximal balloon: (a) cross sectional curve (generatrix), (b) balloon ending (conical sharp corner), (c) balloon body (cylindrical), (d) complete geometrical model of angioplasty balloon, (e) discrete model – 2D shell elements, (f) zoom on the balloon ending

Table 1. Material hyperelastic (Mooney–Rivlin) constants for artery and plague [21]

	Coronary artery	Cellular plague	Calcified plague
a_{10} [MPa]	0.01890	–0.088314	–3.0254
a_{01} [MPa]	0.00275	0.10619	3.1073
a_{20} [MPa]	0.59042	0.11373	107.39
a_{11} [MPa]	0.85718	0.89382	–234.7
a_{02} [MPa]	0	–0.96676	137.22

theory of Mooney–Rivlin, with the material constants experimentally obtained by Prendergast and his team [21]. These values are cited in many papers concerning similar problems [4], [6], [8].

The density of the material was 1.1 $\left[\frac{\text{g}}{\text{cm}^3}\right]$, Poisson's ratio: ν = 0.45 [–]. The equations for the strain energy density function of the material are shown below [15]

$$W(J_1, J_2, J_n) = \sum_{p,q=0}^{n} C_{pq}(J_1 - 3)^p (J_2 - 3)^q + W_H(J) \,. \quad (1)$$

With the 5-parameter M–R model [16]:

$$W = \sum_{p,q=0}^{n} a_{10}(I_1 - 3) + a_{01}(I_2 - 3) + a_{20}(I_1 - 3)^2 + a_{11}(I_1 - 3)(I_2 - 3) + a_{02}(I_2 - 3)^2 . \quad (2)$$

The balloon material model was, as in much of the related research [4], [6], a classical one based on Hooke's theory of elasticity with Young's modulus E = 900 [MPa] and Poisson's ratio ν = 0.3 [–].

2.4. Boundary conditions

For the simulation considered was supposed to be calculated numerically using the implicit method, all the boundary nodes, both from the artery and the balloons, have to be constrained in all possible degrees of freedom (three translational directions and three rotational directions).

The mechanism of contact between the surfaces of the two balloons and the inner wall of the coronary artery was defined by a penalty formulation method (potential areas of contact, indicating the penetrated and penetrating bodies were specified). Optional contact parameters and additional features were used (e.g., small penetration in contact search option, soft constraint formulation, initial penetration check and the IGAP parameter, where the stiffness is not added instantaneously but ramped up to 100% over a certain number of iterations) to improve the convergence of the calculation (implicit methods generate more problems for the contact mechanism than explicit integration methods).

In this case, the contact mechanism was accomplished using the penalty formulation in relation to the normal displacement. To the basic FEM system of equations, based on a stationary functional that represents the sum of the internal energy (deformation of the body) and the potential energy of the external load, a fictional equation of energy in the form of the penalty function is added [15]:

$$\pi(u) = \kappa[(\boldsymbol{B}u - gN)T(\boldsymbol{B}u - gN)] \tag{3}$$

where u describes the global displacement vector, and κ is the stiffness of fictitious spring element acting between two nodes which are in contact. The value of the parameter κ is determined by the accuracy of the computing machine, number of unknowns and the lowest stiffness of elements that are currently in contact or in relation to the masses of bodies remaining in contact using a weight functions [30].

The load was applied as the function of pressure on the inner surface of the two balloons in accordance with given function curves, which are shown in Fig. 3.

2.5. Implicit method – simulation parameters

FEA in static applications is based on the following matrix equation:

$$[K]\{U\} = \{F\} \tag{4}$$

where: $[K]$ – global stiffness matrix of the system (construction stiffness), the sum of the stiffness matrices of individual elements, $\{U\}$ – single-column matrix of the displacements of all nodes, $\{F\}$ – single-column matrix of the loads applied to the nodes of the structure [2].

Due to the nature of the simulations prepared (high nonlinearity while preserving static nature of the issue) it was decided to use the implicit method, specifically the iterative Newton–Raphson scheme. It is a very common method, due to the versatility of its applications and high accuracy of calculations. In each iterative cycle, the full load R is used. In particular cycles, constant, approximate stiffness matrices are assumed, which results in failure to fulfil equilibrium conditions. After each cycle an unbalanced load is acquired in a particular configuration of the deformation. This load is used to determine the additional displacements, which aim at changing the configuration corresponding to the equilibrium configuration [2]:

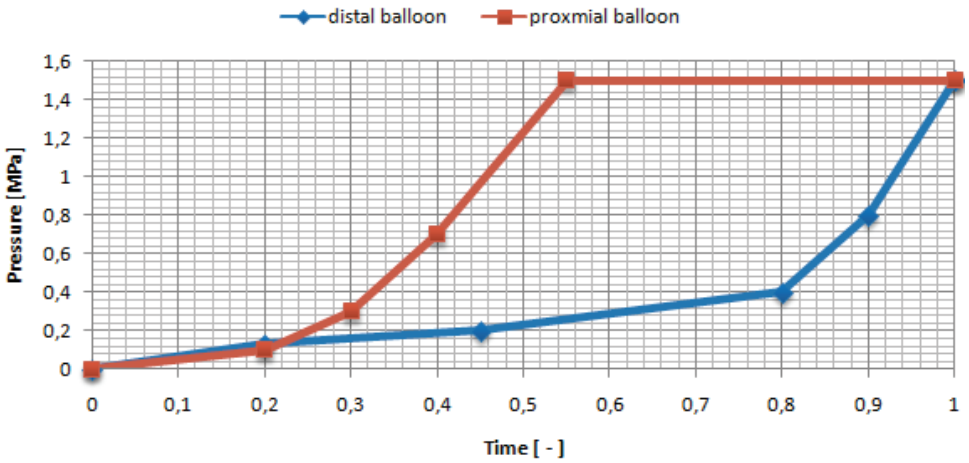

Fig. 3. Functions of the applied pressure throughout the deployment process

$$\Delta r^{(i+1)} = (K_T^{(i)})^{-1} \Delta R^{(i)} \tag{5}$$

where $\Delta r^{(i+1)}$ – increment of displacements in the transition from state i to $i + 1$, K_T – the tangential (approximate) stiffness matrix, $\Delta R^{(i)}$ – unbalanced load ($\Delta R^{(1)}) = R - F^{(1)}$).

The nonlinear numerical solver with BFGS updates (Broyden–Fletcher–Goldfarb–Shanno algorithm), which is the default LS-Dyna solver for nonlinear static analysis, was used. The relative energy and the relative translational displacements of the system were applied as convergence parameters. Automatic time step selection, depending on the number of iterations performed in the previous time step, was defined, which allowed computation time to be shortened and significantly increased the numerical convergence.

Calculations were performed using LSTC LS-Dyna solver. This numerical code is a comprehensive, highly advanced tool for non-linear physical simulations developed by Livermore Software Technology Corporation. It applies the finite element approach and the main mechanism is an explicit integration of dynamic equations of motion.

3. Results

3.1. Simulated procedures

Basic analysis involved simultaneous inflation of both balloons in the modeled fragment of the coronary artery. That is, using some simplifications, an identical process to the "balloon kissing" technique for coronary balloon angioplasty. It is a procedure designed for percutaneous angioplasty of coronary arterial bifurcations, which uses simultaneous inflation of two balloons. One of them is placed in the main branch while the other one is placed partially in the main branch and partially in the side branch. The proximal parts of both balloons touch each other, while the distal parts lay separately [3].

3.2. Numerical results

A deformed shape of the structure studied in four stages – successively at times: $t = 0$ [–] (input structure), $t = 0.2$ [–] (pressure applied to balloons $p = 0.1$ [atm], initial inflation), $t = 0.5$ [–] (pressure applied to proximal balloon = 1.5 [atm]) and $t = 1.0$ [–] (pressure applied to both balloons $p = 1.5$ [atm], the full inflation), is shown in Fig. 4. The coronary artery fragment is shown in a cross section in order to show the balloons inside.

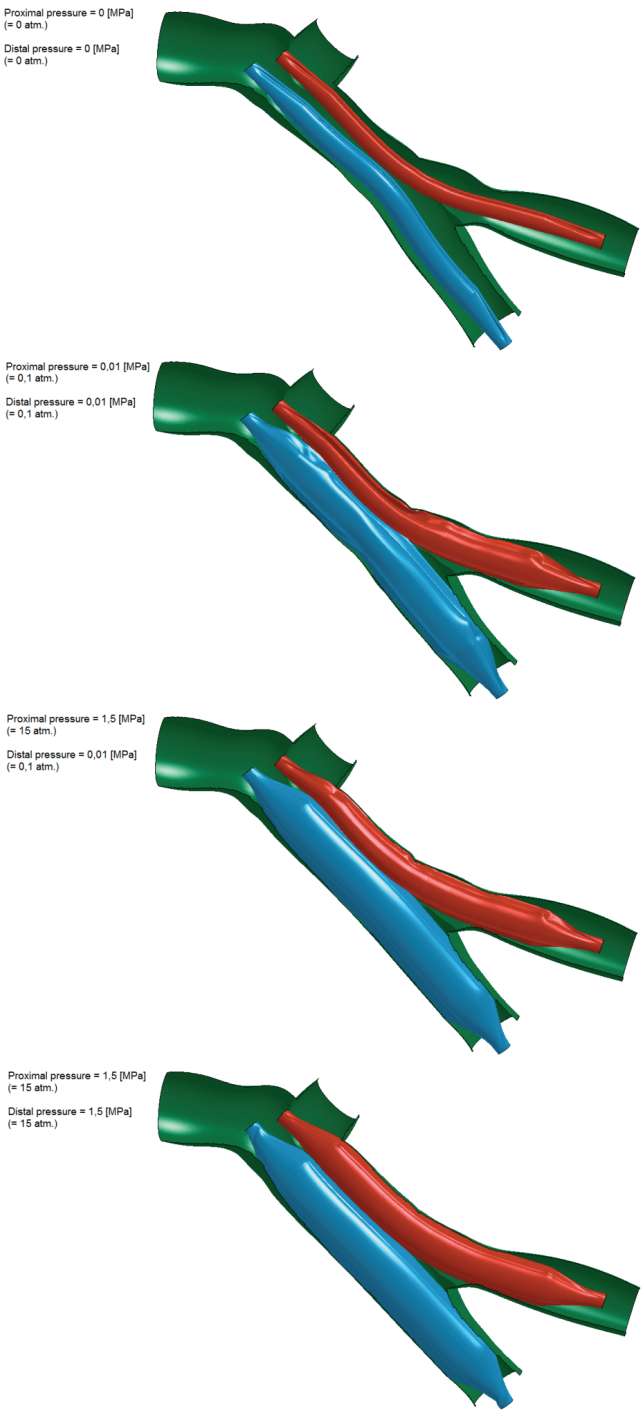

Fig. 4. Simulation of the kissing balloon technique in subsequent stages

The deformed shape of the analyzed structure with applied equivalent tension fringe by the HMH hypothesis (von Mises stress) in four stages – successively at times: $t = 0$ [–] (input structure); $t = 0.2$ [–]

(pressure applied to balloons p = 0.1 [atm], initial inflation); t = 0.5 [–] (pressure applied to proximal balloon = 1.5 [atm]) and t = 1.0 [–] (pressure applied to both balloons p = 1.5 [atm], the full inflation, is shown in Fig. 5.

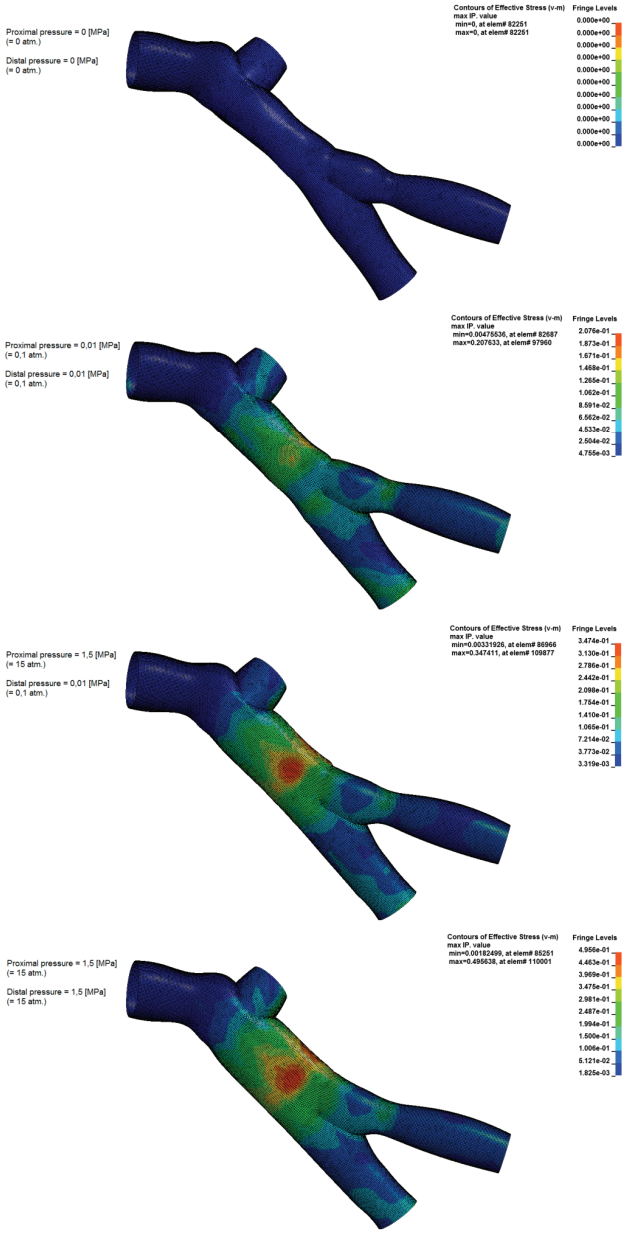

Fig. 5. Arterial wall stress fringes (von Mises) in the kissing procedure inflation

An equivalent tension graph (HMH hypothesis) for a selected finite element of the coronary artery fragment (where intensive balloon contact occurred) versus the pressure applied on balloons throughout the deployment process is shown in Fig. 6.

An issue of applying adequate pressure in the arterial tissue is shown as a graph of relative change for the selected characteristic artery cross sections area, Fig. 7.

4. Discussion

Computer Aided Engineering (CAE) is a branch of technical expertise which appears to be especially useful in biomedical engineering. In particular, analysis performed using various numerical methods [17], [27]. An advanced finite element approach enables simulation of nonlinear problems, characterized by high displacements and deformations, nonlinear material properties and sophisticated contact mechanisms. The relatively low cost of such research methods compared to experiments in vivo (Latin for 'within the living') should also be noted [11]. The applied methods also allow determination of values which, using empirical tests, would be extremely difficult or even impossible to obtain (e.g., the stress or strain rate in specific areas of the model).

Numerical investigations of the inflation process of angioplasty balloons and stents in the coronary arteries using Finite Element Analysis (FEA) were performed on several occasions and it is impossible to mention them all in this short paper. Many of them tackle the major problem of stress distribution in the artery tissue caused by the inflating balloons and stent surfaces [8], [13], [20], [21]. These articles compare amongst others: various stenting techniques, different types of coronary stents [21] or semi-compliant and non-compliant balloons [23]. Additionally, paper [8] presents the distribution of stress compounds in the artery and the emergence of restenosis. Moreover, a numerical analysis of blood flow in the stenosed vessel has been performed [10]. An example of modeling the coronary artery fragment, based on intravascular echo images, can be found in paper [19]. There is also a separate group of papers that describe research on the effects of the applied load on the resulting deformation and stress in the balloon–coronary stent–coronary artery configuration [4], [6]. A certain group of research simulations regarding PTCA surgery in the area of bifurcation [18] focused more on aspect of coronary stents.

The applied methods of data processing led to the development of the coronary artery fragment model, including the arterial bifurcation section. Formed as an actual representation of the geometry of a particular patient's vessel, it may be successfully used as generalization of the artery bifurcation due to sufficiently reproducible linear and angular ratios in whole population.

The process of modeling and simulation of angioplasty non-compliance balloons should be regarded as a success. Numerical simulations presented, in a satisfactory manner, the mechanism of the balloons infla-

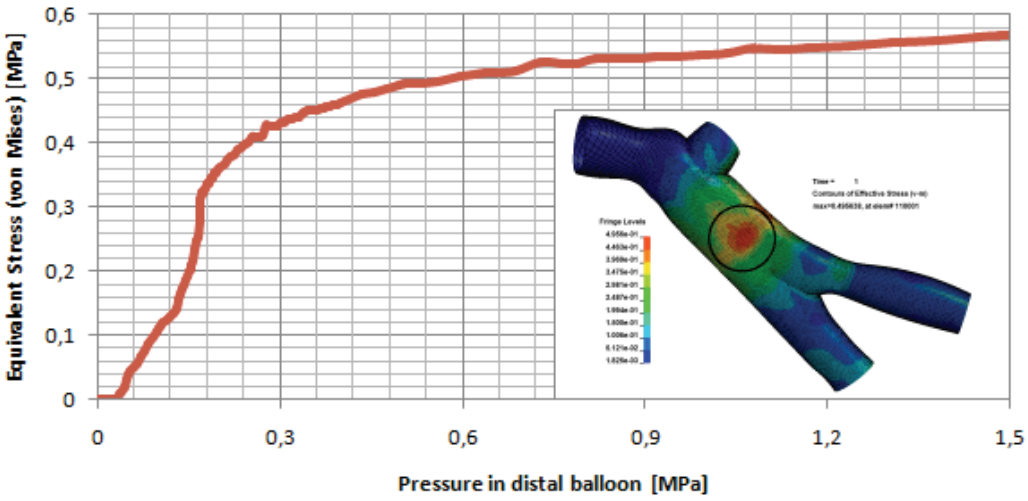

Fig. 6. Equivalent stress (von Mises) in the selected finite element of the coronary artery vs. pressure applied in balloons throughout the deployment process

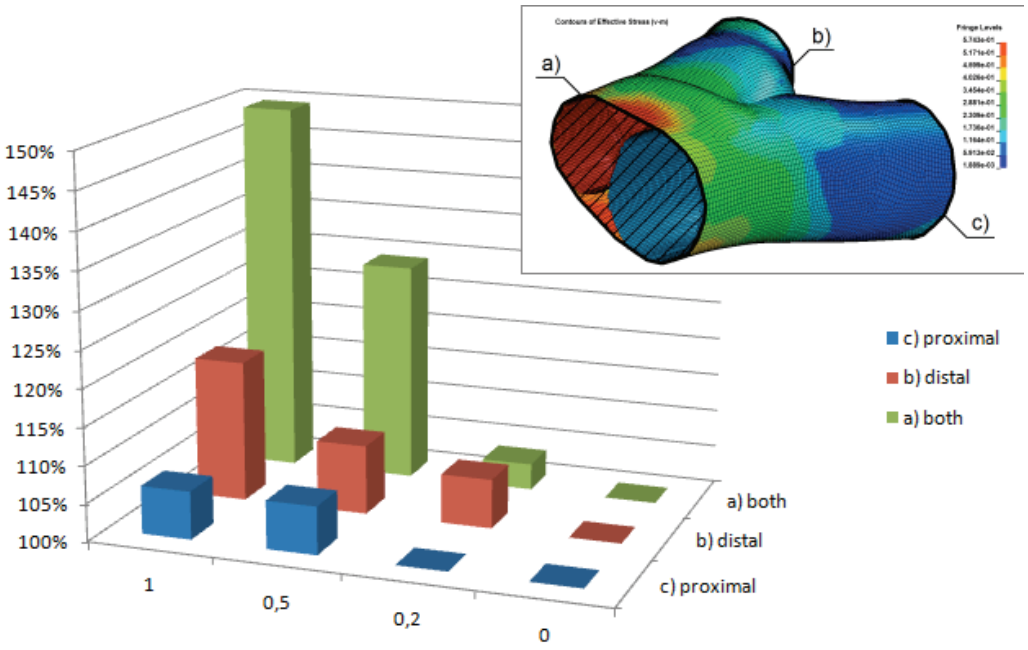

Fig. 7. Relative cross sectional area/time plot for selected sections of the coronary artery

tion and the way the pressure was applied to the vessel walls, confirming most of their advantages (the ability to maintain a predetermined shape and, therefore, to reduce the possibility of damaging the artery).

Measurements of the pressure applied to the coronary vessel walls, illustrated in the graph presented in Fig. 7, as the relative change in the specific area of cross-sections, confirm one of the main disadvantages of the "kissing balloons" method. Excessive pressure applied to the vessel walls is visible in the proximal region of the two cooperating balloons when relatively low pressure act on the proper stenosis (side branch balloon, distal section).

In the authors' opinion, concepts presented in the paper and the analysis performed do not exhaust the topic described and are the basis for further research and development in this area. The authors are absolutely convinced that the elaborated and presented modeling methodology can be extended with case studies of different arteries conditions (certain disease states, etc.) or various equipment configurations. A reference system, in which the results from different arrangements could be compared, was developed. Further research, based on the methodology presented, may lead to valuable insights and specific applications capable of improving the conditions and specifications of coronary angioplasty procedures.

Further works in the presented field are currently being investigated by the authors in cooperation with the medical staff.

Acknowledgements

The study has been supported by the PARP within project No. UDA-POIG.05.01.00-00-013/12-00. This support is gratefully acknowledged.

References

[1] AL SUWAIDI J., BERGER P.B., RIHAL C.S. et al., *Immediate and longterm outcome of intracoronary stent implantation for true bifurcation lesions*, J. Am. Coll. Cardiol., 2000, 35, 929–936.

[2] BELYTSCHKO T., LIU W.K., MORAN B., *Nonlinear Finite Elements for Continua and Structures*, John Wiley & Sons, LTD, England, 2000.

[3] BRUECK M., SCHEINERT D., FLACHSKAMPF F.A., DANIEL W.G., LUDWIG J., *Sequential vs. kissing balloon angioplasty for stenting of bifurcation coronary lesions*, Catheter Cardiovasc. Interv., 2002, 55(4), 461–466.

[4] DE BEULEA M., MORTIER P., CARLIERC S.G., VERHEGGHED B., VAN IMPERA R., VERDONCKB P., *Realistic finite element-based stent design: The impact of balloon folding*, Journal of Biomechanics, 2008, 41, 383–389.

[5] GARRAMONE S., *Structure – Property Relationships in Angioplasty Balloons*, Worcester Polytechnic Institute, May 2001.

[6] GERVASO F., CAPELLI C., PETRINI L., LATTANZIO S., DI VIRGILIO L., MIGLIAVACCA F., *On the effects of different strategies in modelling balloon-expandable stenting by means of finite element method*, Journal of Biomechanics, 2008, 41, 1206–1212.

[7] HOLZAPFEL G.A., SOMMER G., GASSER C.T., REGITNIG P., *Determination of layer-specific mechanical properties of human coronary arteries with nonatherosclerotic intimal thickening and related constitutive modeling*, Am. J. Physiol. Heart Circ. Physiol., 2005, 289, H2048–H2058.

[8] HYRE M.R., PULLIAM R.M., SQUIRE J.C., *Prediction of stent endflare, arterial stresses and flow patterns in a stenotic artery* [Internet], Department of Mechanical Engineering, Virginia Military Institute, USA.

[9] IAKOVOU I., COLOMBO A., *Two-Stent Techniques for the Treatment of Coronary Bifurcations with Drug-Eluting Stents*, Hell J. Cardiol., 2005, 46, 188–198.

[10] JODKO D., OBIDOWSKI D., REOROWICY P., JÓŹWIK K., *Simulations of the blood flow in the arterio-venous fistula for haemodialysis*, Acta of Bioengineering and Biomechanics, 2014, 16(1), 69–74.

[11] KLUESS D., WIEDING J., SOUFFRANT R., MITTELMEIER W., BADER R., *Finite Element Analysis in Orthopaedic Biomechanics* [Internet], University of Rostock, Department of Orthopaedics Rostock, Germany.

[12] KWIATKOWSKI P., GIL R.J., *Angioplastyka z implantacją stentów – powikłania, metody ich unikania i perspektywy leczenia*, Ogólnopolski Przegląd Medyczny, 2012, 4.

[13] LALLY C., DOLAN F., PRENDERGAST P.J., *Cardiovascular stent design and vessel stresses: a finite element analysis*, Journal of Biomechanics, 2005, 38, 1574.

[14] LESIAK M., *Stentowanie bifurkacji tetnic wie}cowych*. Część I. *Dwa naczynia, jeden stent*, Post. Kardiol. Interw., 2009, 4(18), 201–207.

[15] *Livermore Software Technology Corporation*, Ls-Dyna® Keyword Useraş Manual, Vol. II, 2012, version 971, 336.

[16] MAH P., REEVES T.E., MCDAVID W.D., *Deriving Hounsfield units using grey levels in cone beam computed tomography*, Dentomaxillofacial Radiology, 2010, 39, 323–335.

[17] MILENIN A., KOPERNIK M., *Multiscale FEM model of artificial heart chamber composed of nanocoatings*, Acta of Bioengineering and Biomechanics, 2009, 11(2), 13–20.

[18] MORTIER P., DE BEULE M., DUBINI G., HIKICHI Y., MURASATO Y., ORMISTON J.A., *Coronary bifurcation stenting: insights from in vitro and virtual bench testing*, Euro Intervention Supplement, 2010, Vol. 6, J53–J60.

[19] OHAYON J., FINET G., TREYVE F., RIOUFOL G., DUBREUIL O., *A three-dimensional finite element analysis of stress distribution in a coronary atherosclerotic plaque: In-vivo prediction of plaque rupture location*, Biomechanics Applied to Computer Assisted Surgery, 2005, 225–241.

[20] PASZENDA Z., MARCINIAK J., *Biomechanical characteristics of the stent-coronary vessel system*, Acta of Bioengineering and Biomechanics, 2002, 4(1), 81–89.

[21] PRENDERGAST P.J., LALLY C., DALY S., REID A.J. et al., *Analysis of Prolapse in Cardiovascular Stents: A Constitutive Equation for Vascular Tissue and Finite-Element Modelling*, Journal of Biomechanical Engineering, 2003, 125, 699.

[22] ROGERS C., PARIKH S., SEIFERT P., EDELMAN E.R., *Endogenous cell seeding: Remnant endothelium after stenting enhances vascular repair*, Circulation, 1996, 11, 2909–2914.

[23] SCHIEVANO S., KUNZELMAN K., NICOSIA M.A., COCHRAN R.P., EINSTEIN D.R., KHAMBADKONE S., BONHOEFFER P., *Percutaneous Mitral Valve Dilatation: Single Balloon versus Double Balloon. A Finite Element Study*, The Journal of Heart Valve Disease, 2009, 18, 28–34.

[24] SERRUYS P., MORICE M.C., KAPPETEIN A.P. et al., *Percutaneous coronary intervention versus coronary-artery bypass grafting for severe coronary artery disease*, N. Engl. J. Med., 2009, 360, 961–972.

[25] SHAO-LIANG C., IMAD S., *Bifurcation Stents Strategy*, Nanjing First Hospital, Nanjing Medical University, Division of Cardiology, University of Turin.

[26] SIDOROV S., *Finite Element Modeling of Human Artery Tissue with a Nonlinear Multi-Mechanism in Elastic Material*, Dissertation, University of Pittsburgh, 2007.

[27] TYNDYK M.A., BARRON V., MCHUGH P.E., O'MAHONEZ D., *Generation of a finite element model of the thoracolumbar spine*, Acta of Bioengineering and Biomechanics, 2007, 9(1), 35–46.

[28] VASSILEV D., GIL R.J., *Changes in coronary bifurcations after stent placement in the main vessel and balloon opening of stent cell- theory and practical verification on bench – test model*, J. Geriatr. Cardiol., 2008, 5(1), 43–49.

[29] VERHEYE S., GRUBE E., RAMCHARITAR S., SCHOFER J.J. et al., *First-in-man (FIM) study of the Stentys bifurcation stent – 30 days results*, EuroIntervention, 2009, 4(5), 566–571.

[30] VULOVIC S., ZIVKOVIC M., GRUJOVIC N., SLAVKOVIC R., *A comparative study of contact problems solution based on the penalty and Lagrange multiplier approaches*, J. Serbian Society for Computational Mechanics, 2007, 1(1), 174–183.

[31] YAMASHITA T., NISHIDA T., ADAMIAN M.G. et al., *Bifurcation lesions: two stents versus one stent – immediate and follow – up results*, J. Am. Coll. Cardiol., 2000, 35, 1145–1151.